Nitrogen-Doped carbon coated zinc selenide nanoparticles derived from metal−organic framework as high-rate and long-life anode materials for half/full sodium-ion batteries

Yunxiu Wang,[a] Yilin Wang,[b] Zenghui Cai,[a] Zhijiang Yu,[a] Hao Dong,[d] Yifan Zhang,[a] Yanli Zhou,[a] Xintao Zhang,[a] Yanjun Zhai*[c], Fuyi Jiang*[a] and Caifu Dong*[a]

[a] School of Environmental and Material Engineering, Yantai University, Yantai 264005, China.

[b] Trier College of Sustainable Technology, Yantai University, Yantai 264005, China.

[c] School of Chemistry and Chemical Engineering, Liaocheng University, Liaocheng 252059, China.

[d] Shandong Laboratory of Advanced Materials and Green Manufacturing at Yantai, Yantai, 264006, China.

*Corresponding author. E-mail: Yanjun Zhai, zhaiyanjun@lcu.edu.cn; Fuyi Jiang, fyjiang@ytu.edu.cn; Caifu Dong, dongcf@ytu.edu.cn

Keywords: Metal-organic frameworks, ZnSe@NC, sodium ion batteries, anode, long cycle life

Content

Figure captions:

Table S1. Crystal data of compound ZnL.

Compound	ZnL
Chemical formula	$C_{24}H_{17}N_3O_{13}Zn$
Formula weight	620
Crystal system	monoclinic
Space group	P 1 21/n 1
a[Å]	9.0360(9)
b[Å]	8.2692(8)
c[Å]	11.6421(11)
a/b	1.0927
b/c	0.7103
c/a	1.2881
β/[°]	100.926(2)
Volume [$Å^3$]	854.13(14)
Z,Calculated density[Mg/m^3]	4

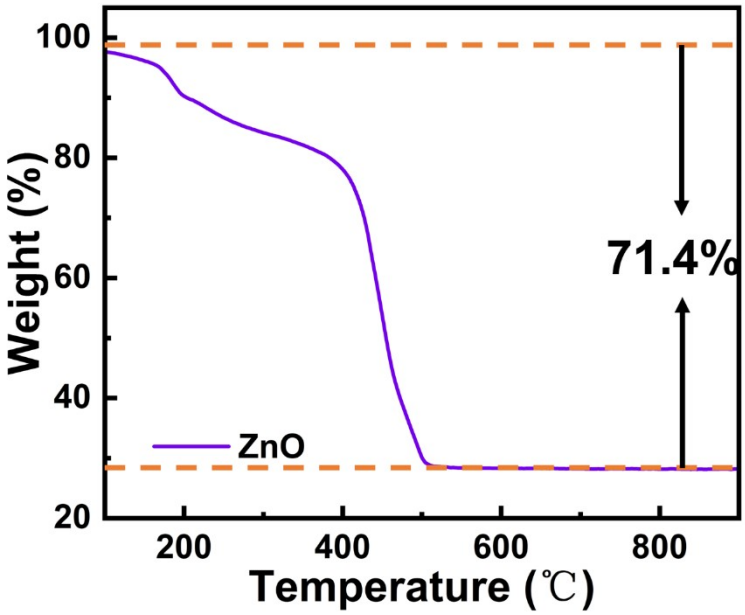

Fig. S1. TGA curve of the ZnL.

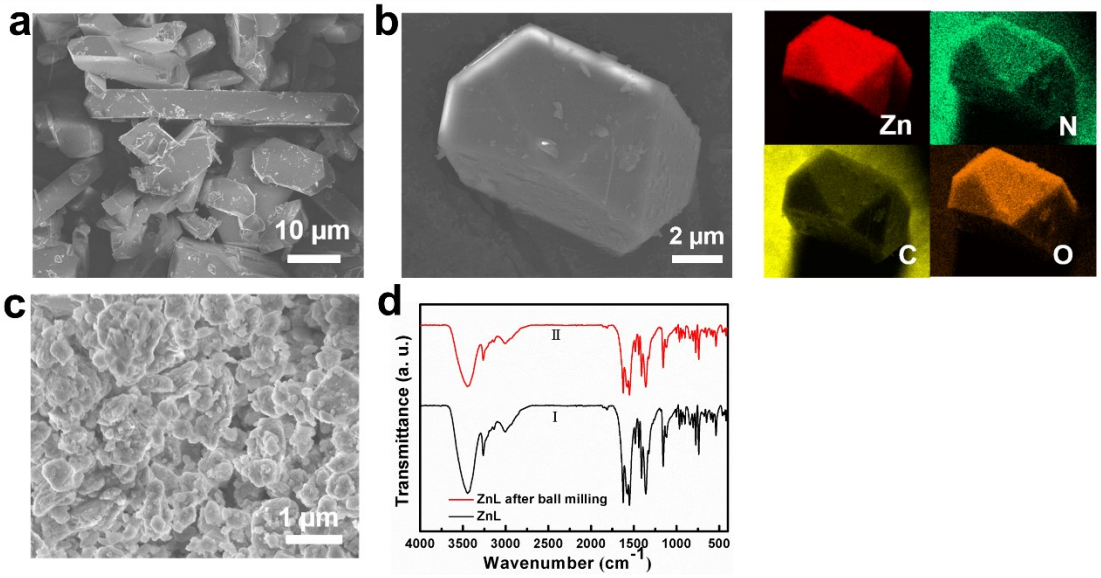

Fig. S2. (a) FESEM image of ZnL. (b) SEM image of ZnL and the corresponding elemental mappings of Zn, N, C and O elements (as labeled). (c) FEEM of ZnL after ball-milling. (d) FT-IR spectra of ZnL before and after ball-milling.

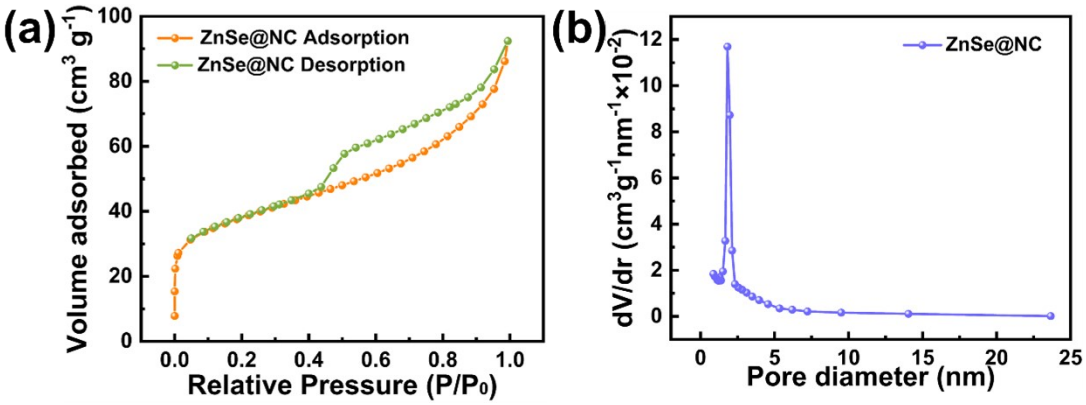

Fig. S3. Nitrogen adsorption–desorption isotherm (a) and the corresponding pore size distribution curve (b) of ZnSe@NC.

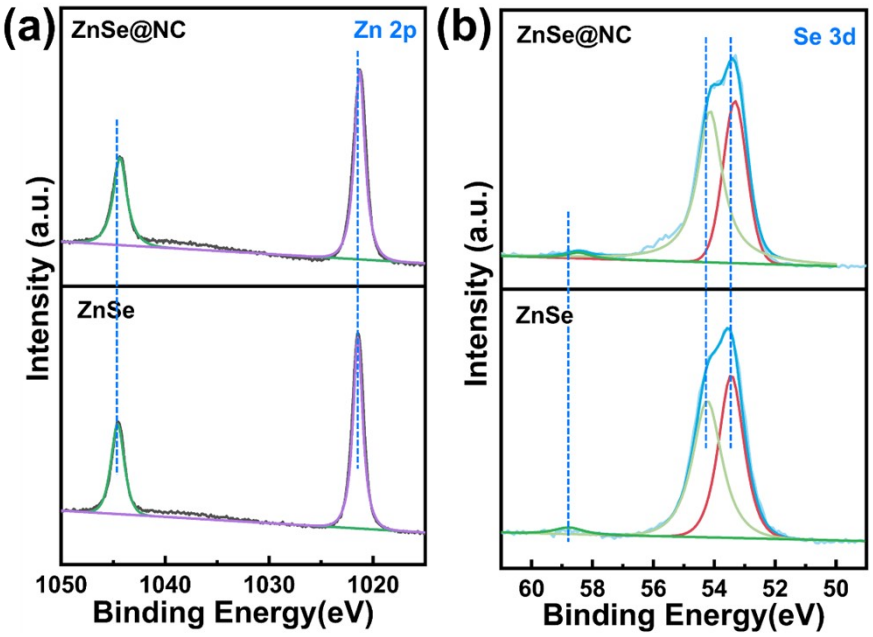

Fig. S4. High resolution XPS spectrum of (a) Zn, (b) Se.

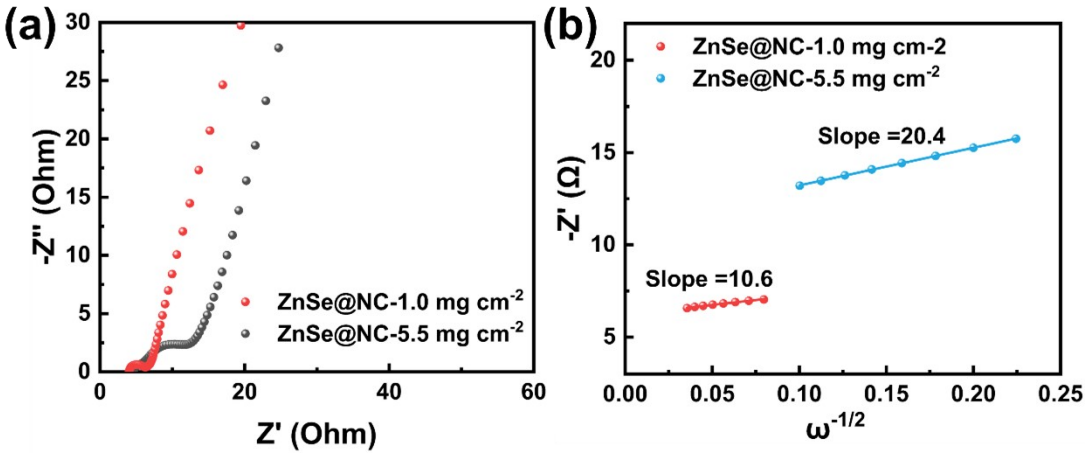

Fig. S5. (a) Nyquist plot of ZnSe@NC at different mass of the active material. (b) The plot of Z' versus $\omega^{-1/2}$ of ZnSe@NC electrode at different mass of the active material.

Table S2. Electrochemical performance comparisons of the ZnSe@NC electrode with those of the previously reported ZnSe for SIBs.

Electrode	Current ($A\ g^{-1}$)	Capacity ($mA\ h\ g^{-1}$)	Cycle number	Initial Coulombic efficiency	Ref/year
ZnSe-rGO	0.1	259.5	50	73.48%	1/2018
ZnSe/HNC	0.5	251.1	500	60.6%	2/2020
ZnSe-rGO	0.1	276.6	100	71.1%	3/2021
ZnSe@C	0.1	284.7	60	71.7%	4/2022
ZnSe@NC/rGO	0.1	365.6	50	45.3%	5/2022
ZnSe@NC NFs	0.1	336.8	150	66.3%	6/2023
ZnSe@CNFs	0.1	241.3	200	69.5%	7/2024
ZnSe-rGO	0.5	323.27	160	71.6%	8/2024
ZnSe@NC	**0.3**	**470.8**	**100**	**81.82%**	**Ourwork**
ZnSe@NC	**4**	**317.6**	**500**	**73.37%**	**Ourwork**

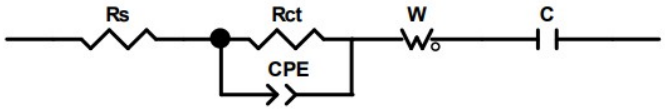

Fig. S6. The equivalent circuit for different number of cycles at open-circuit voltage, 20^{th}, 50^{th}.

Table S3. EIS fitting results of ZnSe@NC at open-circuit voltage, 20 cycles, 50 cycles for SIBs.

Samples	**R_s**	**R_{ct}**
Fresh	3.92	2.045
Cycle-20	3.665	6.641
Cycle-50	4.337	5.643

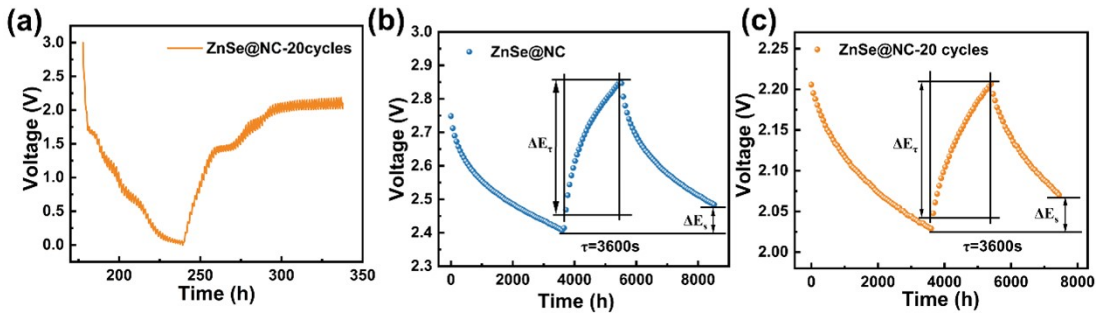

Fig. S7. (a) GITT curves of ZnSe@NC for the 20th cycles. A single GITT titration curve during the charging process of ZnSe@NC for the 4th (b) and 20th (c) cycles.

The GITT test was performed in a voltage range of 0.01−3 V. Prior to GITT measurement, the assembled cells were charged/discharged at 0.2 A g^{-1} for 3 cycles to activate the battery. During the GITT test in the 4th cycle, the cell was charged or discharged at 20 mA g^{-1} for 30 min, then followed by a 60 min open circuit step to allow relaxation back to equilibrium, the procedure was repeated until the charge (or discharge) voltage reached 3.0 V (0.01 V).

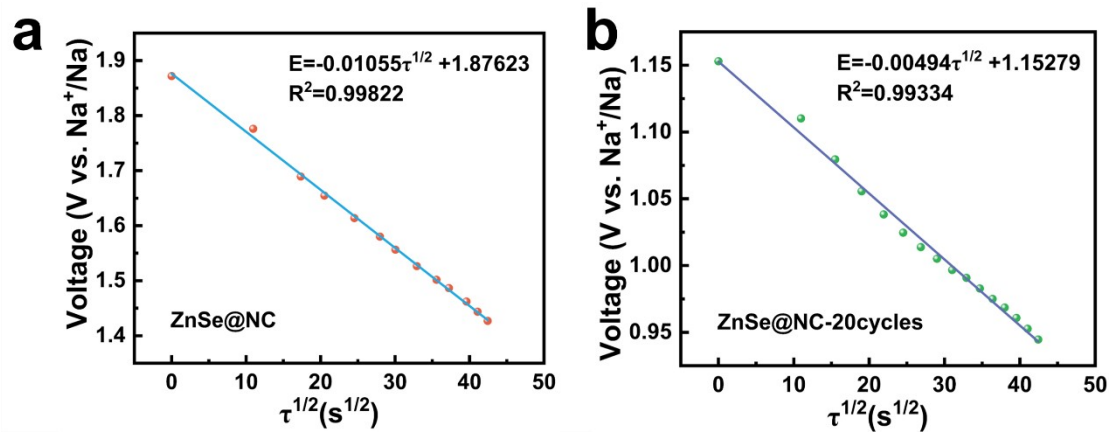

Fig. S8. The plot of voltage vs. root of pulse time ($\tau_{1/2}$) for ZnSe@NC electrodes at different cycles (a) 4th cycle (b) 20th cycle.

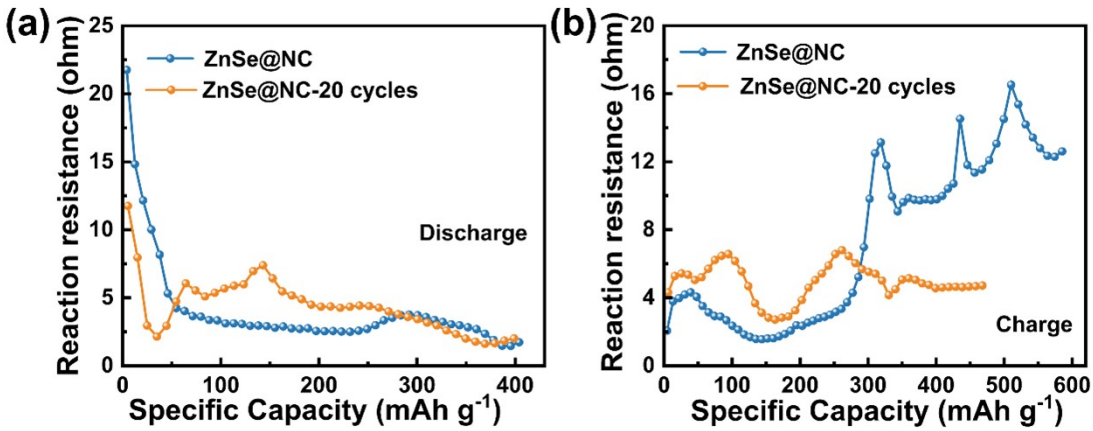

Fig. S9. The reaction impedance during (a) discharge and (b) charge processes.

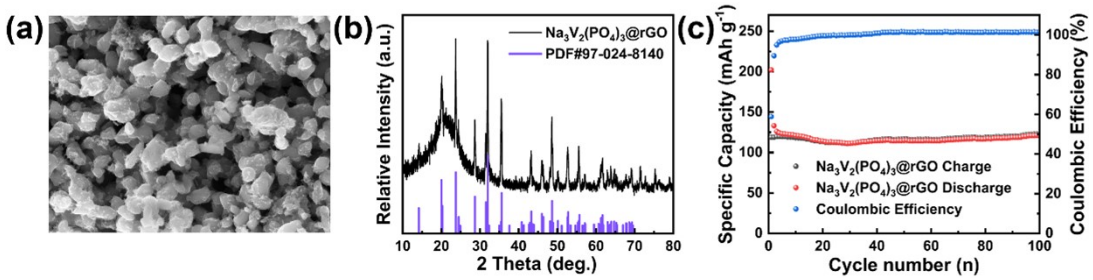

Fig. S10. (a) FESEM image of NVP/rGO. XRD patterns (b) and cycling performance (c) of NVP@rGO at 0.3 A g^{-1}.

References

1 X. Cao, A. J. Li, Y. Yang, and J. T. Chen, ZnSe Nanoparticles Dispersed in Reduced Graphene Oxides with Enhanced Electrochemical Properties in Lithium/Sodium Ion Batteries, *RSC Adv*., 2018, **8**, 25734-25744.

2 M. Jia, Y. H. Jin, C. C. Zhao, P. Z. Zhao, and M. Q. Jia, ZnSe nanoparticles decorated with hollow N-doped carbon nanocubes for high-performance anode material of sodium ion batteries, *J Alloys Compd*., 2020, **831**, 154749.

3 M. Jia, Y. H. Jin, C. C. Zhao, Q. Q. Chang, P. Z. Zhao, H. Wang, and M. Q. Jia, ZnSe with nanostructure embedded in graphene nanosheets with elevated electrochemical performance for anode material of sodium ion battery, *J Alloys Compd*., 2021,**854**, 157318.

4 J. Yuan, J. C. Zhao, T. M. Lu, L. J. Zhang, J. L. Xu, and D. R. Chu, ZnSe@C core-shell microspheres as potential anode material for sodium ion batteries, *Colloids Surf A Physicochem Eng Asp.*, 2022, **641**, 128549.

5 L. T. Zhang, H. G. Zhao, L. M. Dai, F. L. Yao, Y. Huang, W. K. Xue, J. W. Zhu, and J. W. Sun, Rational designed hierarchical dual carbon protected ZnSe anode for advanced sodium-ion hybrid capacitors, *J Energy Storage*, 2022, **52**, 104970.

6. D. Huang, D. X. Wu, J. X. Zhu, J. Y. Xie, J. P. Wu, and J. J. Liang, One-dimensional ZnSe@N-doped carbon nanofibers with simple electrospinning route for superior Na/K-ion storage, *Chin. Chem. Lett.*, 2023, **34**, 107416.

7. B. Y. Liu, L Wang, W. Q. Liu, E. Z. Ren, Z. Y. Wang, Q. Zhang, J. X. Chen, and Y. P. Zeng, In-situ rooting ZnSe nanoparticles in N-doped carbon nanofibers for sodium ion batteries with ultra-long cycle life, *Mater. Lett.*, 2024, **371**, 136931.

8 Y. Jin, H. Seong, J. H. Moon, G. Kim, H. Yoo, T. Jung, S. K. Kim, S. Y. Cho, and J. Choi, Synthesized nanosphere ZnSe and reduced graphene oxide as anode materials for sodium-ion batteries: Analysis on phase transition and storage mechanism, *App. Surf. Sci.*, 2024, **670**, 160606.